# Supplementary Information for:

# Cleavage-furrow formation without F-actin in *Chlamydomonas*

**Masayuki Onishi, James G. Umen, Frederick R. Cross, and John R. Pringle**

This PDF file includes:



www.pnas.org/cgi/doi/10.1073/pnas.1920337117

**Supplementary Materials and Methods**

**Genetic analysis.** Genetic crosses were performed essentially as described previously (1-3). When necessary, segregants were genotyped based on known phenotypes (LatB sensitivity, selectable marker, fluorescence, etc.) or by allele-specific PCR (1) using appropriate primers.

**Plasmids and transformation.** pEB1-mNG (expressing EB1 protein fused to mNeonGreen) was a kind gift from Karl Lechtreck (4). Construction of pMO431 ($P_{H/R}$*:MYO2-CrVenus-3FLAG*) was described previously (5); it expresses MYO2 tagged at its C-terminus with CrVenus-3FLAG from the hybrid *HSP70A/RBCS2* promoter ($P_{H/R}$). All other plasmids used in this study were constructed using one-step isothermal assembly (6); synthetic DNA fragments and primers were obtained from Integrated DNA Technologies. All plasmids and corresponding sequence files are available through the Chlamydomonas Resource Center (https://www.chlamycollection.org). pMO654 ($P_{H/R}$*:Lifeact-mNG*) was constructed by replacing *CrVenus-3FLAG* in pMO459 (7) with *mNG* from pEB1-mNG. A similar replacement of $P_{TUB2}$ and *CrVenus* in pMO561 (7) with $P_{H/R}$ and *mNG* yielded pMO665 ($P_{H/R}$*:mNG-3FLAG*), and genomic DNA sequences of the *PMH1* (Cre03.g164600), *MYO1* (Cre16.g658650), and *MYO3* (Cre13.g563800) coding regions (start codon to last coding codon, including all introns) were inserted into the *Hpa*I site of pMO665 to generate pMO683 ($P_{H/R}$*:PMH1-mNG-3FLAG*), pMO668 ($P_{H/R}$*:MYO1-mNG-3FLAG*), and pMO669 ($P_{H/R}$*:MYO3-mNG-3FLAG*), respectively. Transformation by electroporation was done using a NEPA21 square-pulse electroporator and CHES buffer, as described previously (7), and transformants with strong Venus or mNG expression were identified by screening using a Tecan Infinite 200 PRO microplate reader at excitation and emission wavelengths of 515 and 550 nm, as described previously (7). Paromomycin (Sigma or EMD Millipore) and Zeocin (InvivoGen) were used at 10 µg/ml to select for and maintain strains that were transformed with constructs containing resistance markers.

**Light microscopy.** Fluorescence and DIC microscopy of cells expressing Venus-, mNG-, and/or GFP-tagged proteins was performed as follows. Cells were mounted on a thin pad of TAP medium containing 1.5% low-melting-point agarose (Invitrogen) and sealed with a coverslip and VALAP. When desired, LatB was added to the agarose-containing medium at 3 µM. The cells were observed using a Nikon Eclipse 600-FN microscope equipped with an Apochromat 100X/1.40 N.A. oil-immersion objective lens, an ORCA-2 cooled CCD camera (Hamamatsu Photonics), and Metamorph version 7.5 software (Molecular Devices). Signals of all fluorescent proteins were captured using YFP filters; chlorophyll autofluorescence was captured using Texas Red filters. For time-lapse experiments, the stage temperature was maintained at ~26°C using a heater (AmScope), and the slide was continuously illuminated by red LED lights to support photosynthesis. The distance from the leading edge of the cleavage furrow to the opposite side of the cell was determined at each time point to provide an approximate quantitative measure of the progress of furrow ingression. To visualize the rates of furrow ingression, local polynomial regression curves were generated using the LOESS (locally estimated scatterplot smoothing) method, and means and 95% confidence intervals of 1000 such curves were calculated using the loess.boot() function in the R package spatialEco. Images were post-processed using ImageJ (National Institutes of Health) and Photoshop (Adobe) software. Images from a single experiment with a single strain were processed identically and can be compared directly in the Figures.

The bright-field images in Fig. 4A and Fig. S3D were captured using a Leica DMI 6000 B

microscope equipped with a 40X objective lens and Leica DFC 450 camera. Cell-wall removal by autolysin was performed essentially as described previously (8).

**Western blotting.** Whole-cell extracts were prepared as described previously (9). SDS-PAGE was performed using Tris-glycine gels (8% for myosins, 11% for actin). After the proteins were transferred onto PVDF membranes, the blots were stained with a mouse monoclonal anti-FLAG (Sigma, F1804) or anti-actin (clone C4, EMD Millipore, MAB1501) antibody, followed by an HRP-conjugated anti-mouse-IgG secondary antibody (ICN Pharmaceuticals, 55564).

**Phylogenetic analysis.** The amino-acid sequences of all myosins in the genomes of *Chlamydomonas* (MYO1, Cre16.g658650.t1.1; MYO2, Cre09.g416250.t1.1; MYO3, Cre13.g563800.t1.1 from Phytozome v5.5: phytozome.jgi.doe.gov), *Arabidopsis thaliana* (10), *D. melanogaster* (10), and *S. cerevisiae* (Myo1, YHR023W; Myo2, YOR326W; Myo3, YKL129C; Myo4, YAL029C; Myo5, YMR109W from Saccharomyces Genome Database: www.yeastgenome.org) were aligned using ClustalW 2.1 and the BLOSUM62 matrix. This alignment was then used to generate an unrooted Maximum Likelihood tree with approximate likelihood test using the VT model in PhyML (11).

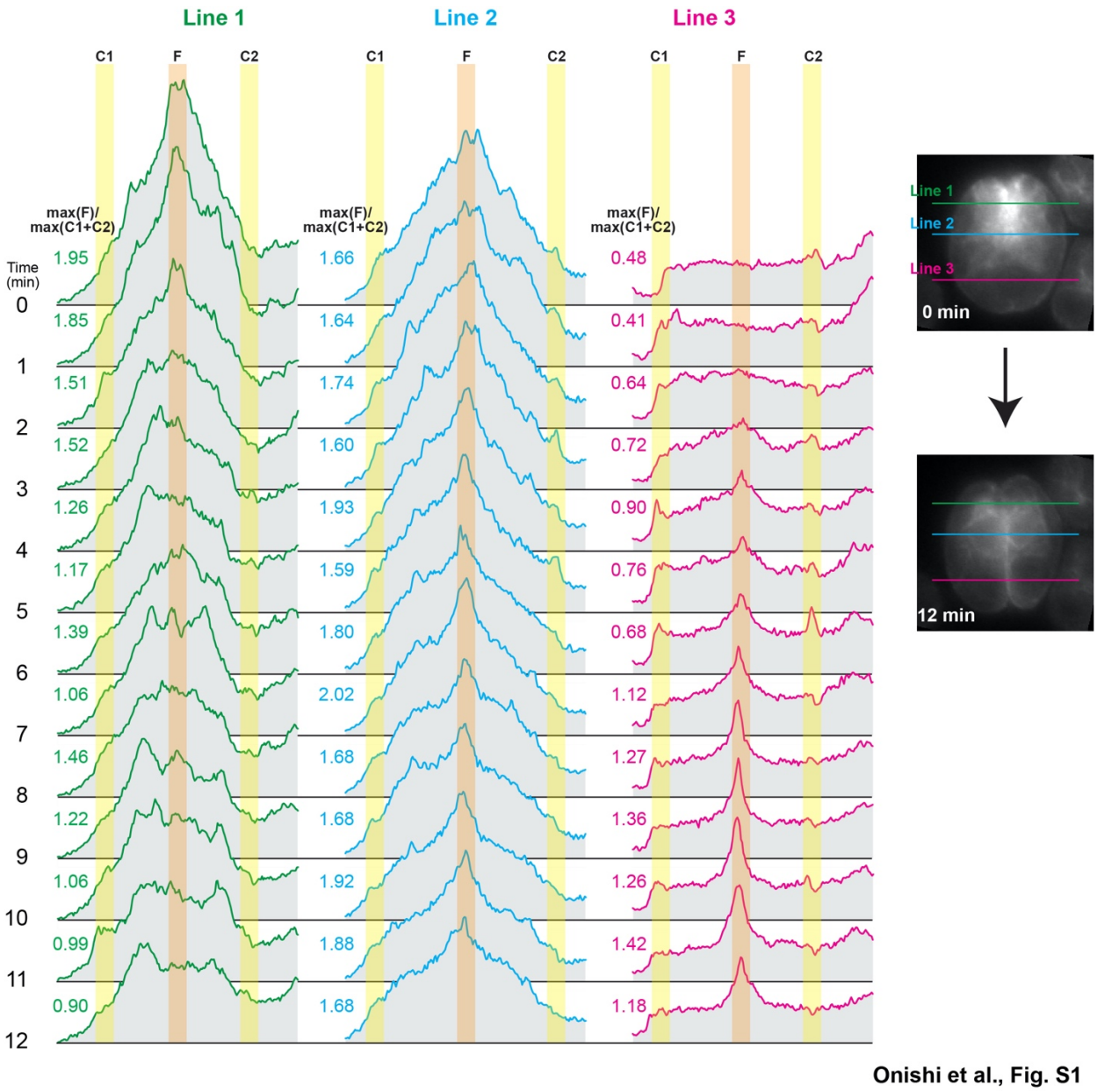


**Fig. S1.** Evidence for enrichment of F-actin in the furrow region. Line-scan quantification of Lifeact-mNG fluorescence intensity were performed at three positions along the anteroposterior axis on the images from the time-lapse series shown in Fig. 2B. The ratios of the maximum furrow signal (F) to the sum of the maximum cortical signals (C1 and C2) are shown.

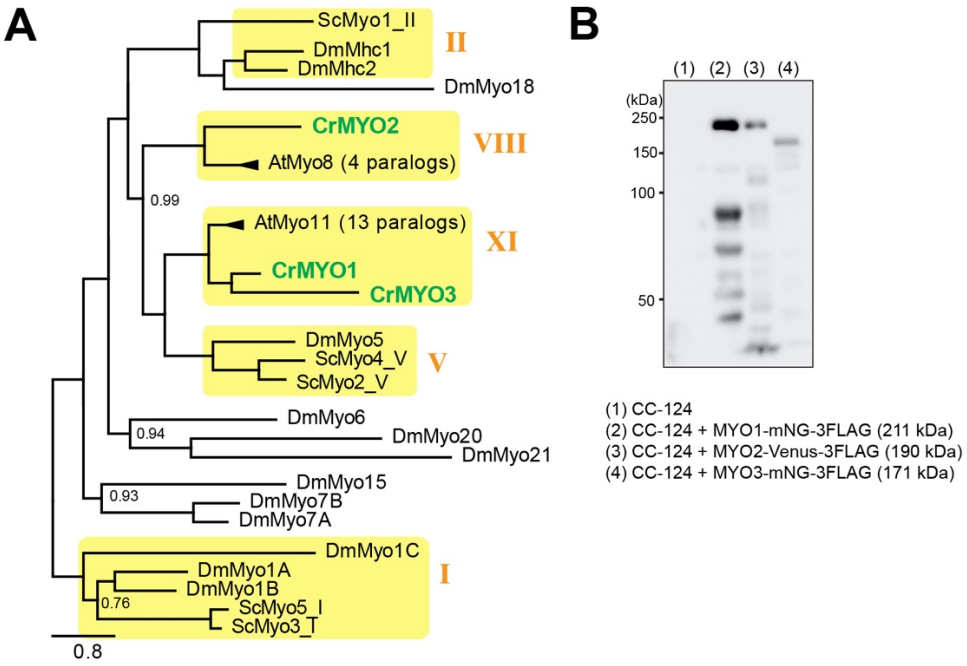


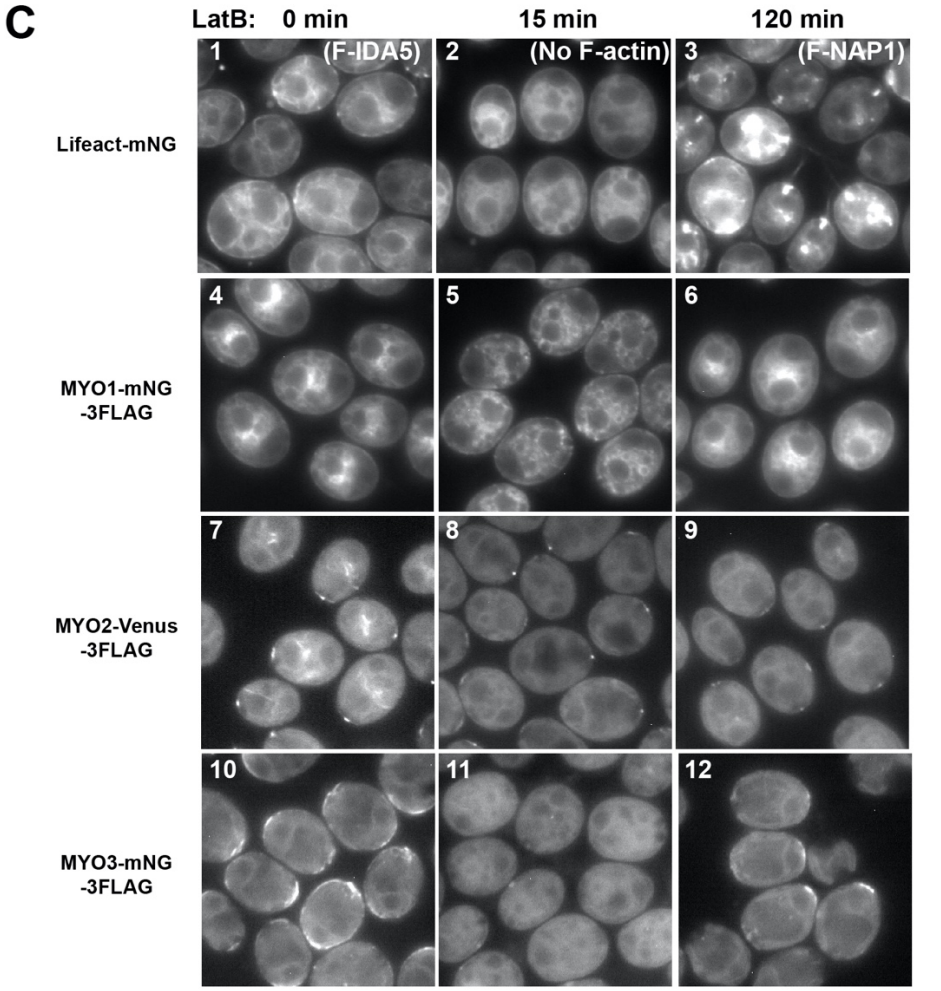


Onishi et al., Fig. S2

**Fig. S2.** (*A*) Maximum-likelihood tree of amino-acid sequences of all myosins from *D. melanogaster* (Dm), *S. cerevisiae* (Sc), *A. thaliana* (At), and *C. reinhardtii* (Cr). Three *Chlamydomonas* myosins (green) clustered with plant-specific type-VIII and type-XI myosins. Scale bar, substitutions per residue. Branch supports below 1.0 are shown next to nodes. See Materials and Methods for details. (*B*) Expression of mNG-3FLAG-tagged or Venus-3-FLAG-tagged myosins. Whole-cell extracts from wild-type (CC-124) and transformed cells were analyzed by Western blotting using an anti-FLAG antibody. The positions of molecular-weight markers are indicated on the left and the predicted molecular weights of the tagged proteins are indicated in the lane descriptions below. (*C*) Response of F-actin and the tagged myosins to LatB treatment. Cells expressing Lifeact-mNG (1-3) or a tagged myosin (4-12) were treated with 10 μM LatB for the indicated times. See text for details.

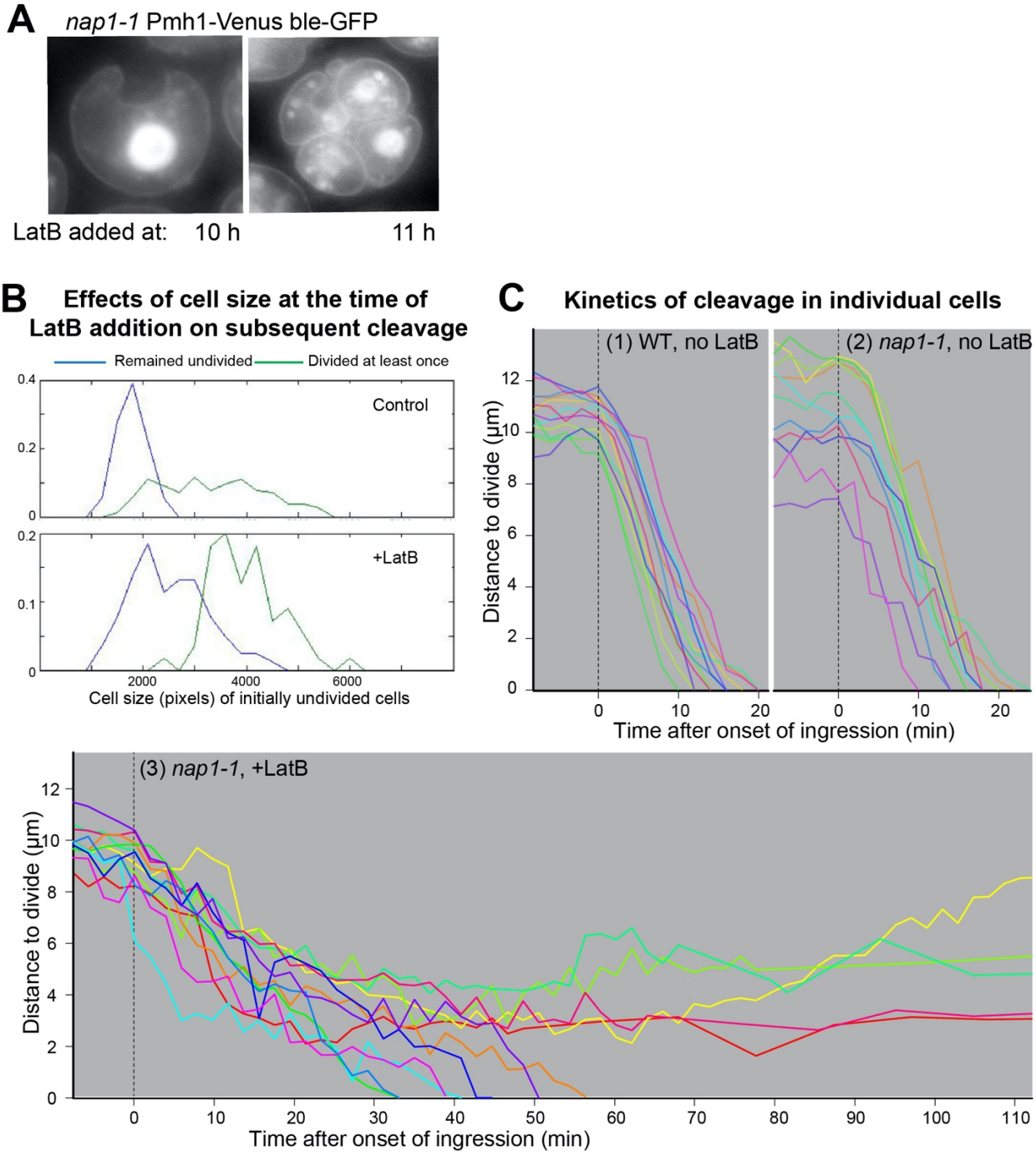


**Onishi et al., Fig. S3**

**Fig. S3.** (*A*) Failure of mitosis when F-actin is eliminated sufficiently early in the cell cycle. In an experiment like that of Fig. 4*A*, *nap1-1* cells expressing PMH1-Venus and the nuclear marker ble-GFP were treated with 3 μM LatB beginning at the indicated times and imaged at 20 h. (*B*) Correlation between cell size and successful formation of furrows in the absence of F-actin. *nap1-1* cells were synchronized using the -N method (see Materials and Methods). At 11 h, as the first cells began to divide, the cells were transferred to fresh plates with or without 3 μM LatB and imaged every 30 min by brightfield microscopy. The fractions of individual cells that divided successfully were plotted as a function of the size of the cells at the time of transfer. (*C*) The kinetics of cleavage in individual cells in the experiments of Fig. 5. The lack of smoothness of the lines in panels 2 and 3 results from imaging noise caused by the unstable autofocus. (*D*) Additional evidence for an abscission defect in cells lacking F-actin. In the experiment of Fig. 4*A*, control cells and cells treated with LatB beginning at 11 h were examined at 20 h. Cells were treated with autolysin before examination (see Materials and Methods). Control cells became rounder than normal as a result of cell-wall removal. ~5% of the LatB-treated cells remained connected by narrow intercellular bridges, as shown here in two representative cells.

## Legends for Supplemental Movies

Movie S1. A dividing wild-type cell expressing PMH1-mNG. Selected frames are shown in Fig. 1A.

Movie S2. A roughly synchronized population of wild-type cells expressing PMH1-mNG.

Movie S3. A dividing *nap1-1* cell expressing PMH1-mNG. Selected frames are shown in Fig. 5A.

Movie S4. A dividing *nap1-1* cell expressing PMH1-mNG that had been pretreated with 3 μM LatB. Selected frames are shown in Fig. 5B (1).

Movie S5. A dividing *nap1-1* cell expressing PMH1-mNG that had been pretreated with 3 μM LatB. Selected frames are shown in Fig. 5B (2).

Movie S6. A dividing *nap1-1* cell expressing PMH1-mNG that had been pretreated with 3 μM LatB. Selected frames are shown in Fig. 5B (3).

Movie S7. A dividing *nap1-1* cell expressing EB1-mNG. Selected frames are shown in Fig. 6A.

Movie S8. A dividing *nap1-1* cell expressing EB1-mNG that had been pretreated with 3 μM LatB. Selected frames are shown in Fig. 6B.

**SI References**


1. M. Onishi, J. R. Pringle, F. R. Cross, Evidence that an unconventional actin can provide essential F-actin function and that a surveillance system monitors F-actin integrity in *Chlamydomonas*. *Genetics* **202**, 977-996 (2016).
2. S. K. Dutcher, "Mating and tetrad analysis in *Chlamydomonas reinhardtii*" in Methods in Cell Biology, W. Dentler, G. Witman, Eds. (Academic Press, 1995), vol. 47, pp. 531-540.
3. F. Tulin, Mating and tetrad dissection in *Chlamydomonas*. *Bio-101*, e3207 (2019).
4. J. A. Harris, Y. Liu, P. Yang, P. Kner, K. F. Lechtreck, Single-particle imaging reveals intraflagellar transport-independent transport and accumulation of EB1 in *Chlamydomonas* flagella. *Mol. Biol. Cell* **27**, 295-307 (2016).
5. P. Avasthi *et al.*, Actin is required for IFT regulation in *Chlamydomonas reinhardtii*. *Curr. Biol.* **24**, 2025-2032 (2014).
6. D. G. Gibson *et al.*, Enzymatic assembly of DNA molecules up to several hundred kilobases. *Nat Methods* **6**, 343-345 (2009).
7. M. Onishi, J. R. Pringle, Robust transgene expression from bicistronic mRNA in the green alga *Chlamydomonas reinhardtii*. *G3 (Bethesda)* **6**, 4115-4125 (2016).
8. S. K. Dutcher, Purification of basal bodies and basal body complexes from *Chlamydomonas reinhardtii*. *Methods Cell Biol.* **47**, 323-334 (1995).
9. M. Onishi, K. Pecani, T. Jones IV, J. R. Pringle, F. R. Cross, F-actin homeostasis through transcriptional regulation and proteasome-mediated proteolysis. *Proc. Natl. Acad. Sci. U. S. A.* **115**, E6487-E6496 (2018).
10. F. Odronitz, M. Kollmar, Drawing the tree of eukaryotic life based on the analysis of 2,269 manually annotated myosins from 328 species. *Genome Biol.* **8**, R196 (2007).
11. S. Guindon *et al.*, New algorithms and methods to estimate maximum-likelihood phylogenies: assessing the performance of PhyML 3.0. *Syst. Biol.* **59**, 307-321 (2010).